ELSEVIER

Journal of Power Sources 90 (2000) 76–81

JOURNAL OF POWER SOURCES

www.elsevier.com/locate/jpowsour

Lithium nickelate electrodes with enhanced high-temperature performance and thermal stability

Hajime Arai *, Masayuki Tsuda, Yoji Sakurai

NTT Telecommunications Energy Laboratories, Tokai, Ibaraki 319-1193, Japan

Received 14 November 1999; received in revised form 25 January 2000; accepted 10 February 2000

Abstract

Lithium nickelate is an attractive positive electrode material for lithium ion batteries because of its large capacity at ambient temperatures. However, highly delithiated $LiNiO_2$ (e.g. $Li_{0.2}NiO_2$) shows undesirable exothermal heat at 200°C. We found another issue of $LiNiO_2$ in this study, namely poor reversibility at 40°C. To overcome these disadvantages, we introduced cobalt, manganese, and titanium as partial substituents for nickel. Cobalt substitution was effective in improving the reversibility at 40°C. The exothermal decomposition of the delithiated compounds was suppressed by using manganese and titanium as substituents. We found doubly substituted nickelate $LiNi_{0.8}Co_{0.1}Ti_{0.1}O_2$ to be the most promising in terms of large capacity (190 mA h g^{-1}), enhanced high-temperature performance, and improved thermal stability.

Keywords: Lithium nickelate; Positive electrode material; Lithium ion battery; Substitution; High-temperature performance; Thermal stability

1. Introduction

Lithium nickelate is an attractive positive electrode material for lithium ion batteries because of its comparatively low cost and large capacity [1,2]. $LiNiO_2$ with a well-defined layered structure provides a cycle capacity of over 200 mA h g^{-1} [3–11]. Most of the lithium in layered $LiNiO_2$ is extracted at a moderately positive potential, for example at 4.3 V vs. Li/Li^+. This characteristic gives the large capacity but also produces highly delithiated (lithium extracted) states which can reduce the stability of the material. It has been reported that the highly delithiated compound $Li_{1-y}NiO_2$ ($y \geq 0.7$) decomposes exothermally at around 200°C [12–17] while lithium cobaltate obtained at the same potential, $Li_{1-y}CoO_2$ with $y \sim 0.5$, is stable at 200°C [12,16]. Also the question is the reversibility of nickelate electrodes at higher than ambient temperatures because the material at higher degrees of delithiation is thermodynamically metastable and might be degraded at high operating temperatures. A substitution technique seems to be the key to overcoming these disadvantages [13,18,19].

In this study, we describe the high-temperature performance and thermal behavior of $LiNiO_2$ and its substituted compounds. Cobalt, manganese and titanium were used for the substituents. We report a material which exhibits enhanced high-temperature performance and thermal stability while maintaining a large reversible capacity of 190 mA h g^{-1}.

2. Experimental

We used reagent grade $LiOH \cdot H_2O$, $LiNO_3$ (1:1 mixture) and $Ni(OH)_2$ (Kanto Chemical) to prepare all the samples. Co_3O_4, MnO, and TiO (Kanto Chemical) were added as needed. The transition metal reactants were used in the same stoichiometric ratio as in the target material. We used double the stoichiometric amount of lithium so that the transition metal in the lithium predominant layer was minimized [8]. For example, the molar ratio of the reactant mixture was Li:Ni:Co:Ti = 20:8:1:1 when we prepared $LiNi_{0.8}Co_{0.1}Ti_{0.1}O_2$. The mixture was heated in air at 500°C for 6 h and then at 700°C for 24 h. We washed the obtained powder with distilled water to remove unre-

* Corresponding author. Fax: +81-29-270-4095.
E-mail address: arai@iba.iecl.ntt.co.jp (H. Arai).

0378-7753/00/$ - see front matter
PII: S0378-7753(00)00451-1

acted lithium compounds. We then dried it at 100°C for more than 12 h.

We characterized the structure of the compound by X-ray diffraction (Rigaku RU-200, RAD-rX) with Cu Kα radiation. Rietveld analysis was performed with the aid of the computer program RIETAN [20]. We assumed a structure of $[Li_{1-x}(TM)_x]_{3b}[(TM)_{1-w}Li_w]_{3a}[O_2]_{6c}$ ($x < 0.5$ and $w < 0.5$) with a space group R3m and a hexagonal setting, where the transition metals (denoted as TM) form a solid solution in the compound. 3b and 3a sites correspond to lithium and transition metal predominant layers, respectively. The average scattering factor of TM was used to calculate the structure factor.

We conducted electrochemical measurements at 20°C and 40°C using coin-type cells [8] equipped with a metallic lithium counter electrode and a 1-M $LiPF_6$ electrolyte solution in equal volumes of ethylene carbonate and dimethyl carbonate. The working electrode mixture consisted of the nickelate material (70 wt.%), acetylene black (Denki Kagaku) (25 wt.%) and polytetrafluoroethylene (Daikin) (5 wt.%). The quasi open circuit voltage (QOCV) profiles were measured by applying an intermittent current of 0.1 mA cm^{-2} for 2 h followed by a 2-h rest. Unless otherwise mentioned, we stopped the charging test at a closed circuit (current flowing) voltage of 4.5 V before starting the following discharging test. A single charging test typically took 2 weeks. We estimate the lithium content of the charge–discharge compounds using the transferred charge and the weight of the electrode material. We performed constant current charge–discharge (cycle) tests in a 3.0- to 4.3-V range at 0.5 mA cm^{-2}.

We measured the thermal behavior of the delithiated compounds using differential scanning calorimetry (DSC) (Rigaku TAS-100) in an argon atmosphere at a heating rate of 10°C min^{-1}. The delithiated compound was prepared by electrochemical delithiation at 0.1 mA cm^{-2} followed by a relaxation period of 1 week in the cell. The electrode mixture was taken from the cell, washed with tetrahydrofuran, dried in a vacuum, and part of it (approximately 5 mg) was used for the DSC measurement. We measured the behavior up to 300°C where acetylene black and polytetrafluoroethylene are stable [15].

3. Results and discussion

3.1. Structural characteristics

The observed X-ray patterns were all similar to that of layered $LiNiO_2$ and no other phase was detected. Table 1 shows the structural parameters of the compounds analyzed by the Rietveld method. The nominal chemical composition of the target material is used in Table 1 and hereafter. The calculated pattern we obtained by the Rietveld analysis provided a good fit with the experimentally observed pattern, indicating that the proposed structural model is appropriate. Typical R_{wp} and R_I values from the Rietveld analysis [20] were 10 and 2, respectively.

The x value is small in all the samples in Table 1, namely, there was little transition metal contamination in the lithium predominant layer. This result indicates that the method we used here for preparation is useful for preparing layered lithium nickelate in air. The cobalt substituted compounds have a well-defined layered structure with a smaller x value than $LiNiO_2$, as previously reported [21–23]. This suggests that the transition metal found in the lithium predominant layer is nickel (Ni^{2+}) and cobalt exists only in the 3a site.

The substituted compounds containing manganese and titanium showed positive w values, which reveals that lithium is found in the transition metal predominant layer. The error in the w value was large due to the small scattering factor of lithium, nevertheless, the R_{wp} and R_I values were certainly reduced by introducing a positive w value for compounds containing manganese and titanium as the substituent. We found no such tendency for $LiNiO_2$ and $LiNi_{0.9}Co_{0.1}O_2$. Chemical analysis of manganese-substituted lithium nickelate has shown that the lithium ratio to transition metal tends to be over unity and

Table 1
Structural parameters and rechargeable capacity of nickelate compounds

Compound name[a]	a (Å)	c (Å)	z (O)	x[b]	w[b]	Cycle capacity at 20°C (mA h g^{-1})[c]
$LiNiO_2$	2.8739(1)	14.186(1)	0.259(2)	0.01(1)	0[d]	210
$LiNi_{0.9}Co_{0.1}O_2$	2.8685(1)	14.170(1)	0.259(2)	0.01(1)	0[d]	200
$LiNi_{0.9}Mn_{0.1}O_2$	2.8709(1)	14.179(1)	0.259(1)	0.03(1)	0.04(2)	185
$LiNi_{0.9}Ti_{0.1}O_2$	2.8766(1)	14.215(1)	0.259(1)	0.02(1)	0.04(2)	185
$LiNi_{0.8}Co_{0.1}Mn_{0.1}O_2$	2.8645(1)	14.161(1)	0.259(1)	0.02(1)	0.05(2)	175
$LiNi_{0.8}Co_{0.1}Ti_{0.1}O_2$	2.8753(1)	14.215(1)	0.259(2)	0.02(1)	0.05(2)	190

[a] Nominal chemical composition of the target material (see text).
[b] A formula of $[Li_{1-x}(TM)_x]_{3b}[(TM)_{1-w}Li_w]_{3a}[O_2]_{6c}$ was assumed where TM denotes transition metals (see text).
[c] Data at 0.5 mA cm^{-2}, cycled between 3.0 and 4.3 V.
[d] This term was fixed to be zero because no positive value was obtained.

that manganese ions exist partly as Mn(IV) [24–26]. We believe, based on these facts, that the manganese-substituted lithium nickelate consist of solid solutions of $[Li]_{3b}[Ni_{1-z}Mn(III)_z]_{3a}[O_2]_{6c}$ and $[Li]_{3b}[Li_{1/3}Mn(IV)_{2/3}]_{3a}[O_2]_{6c}$ (or Li_2MnO_3). We deduce that a similar solid solution is also formed for titanium-substituted lithium nickelate, because Ti (IV) is more stable than Ti(III) and easily forms $Li[Li_{1/3}Ti_{2/3}]O_2$ (or Li_2TiO_3). If manganese and titanium exist with valences of +3 and +4, their ionic radii and positive charges are too far from those of Li^+ and they may only be accommodated in the 3a site.

The doubly substituted system $LiNi_{0.8}Co_{0.1}M_{0.1}O_2$ (M = Mn, Ti) showed both the structural features observed in cobalt- and manganese-substituted compounds, namely small x values and positive w values.

3.2. Characteristics of $LiNiO_2$

The non-substituted $LiNiO_2$ provided a large cycle capacity at 20°C as shown in Table 1. It turned out, however, that the reversibility is poor at higher than ambient temperatures. Figs. 1 and 2 show the QOCV profiles of $Li_{1-y}NiO_2$ during the first charge–discharge cycle measured at 20°C and 40°C, respectively. There was similarity in the voltage profiles during charging and discharging with approximately 80% of the material (corresponding to 220 mA h g^{-1}) being active at 20°C. Considerable irreversibility was observed at 40°C with a loss of the voltage region over 4 V in Fig. 2. When the charging process was stopped at $Li_{0.2}NiO_2$ followed by discharging, the reversibility was good at 40°C as shown in Fig. 3, as well as at 20°C [11]. However, it is practically difficult to control the degree of delithiation around $Li_{0.2}NiO_2$ by means of voltage detection, because there is a voltage plateau at 4.15 V (see Figs. 1 and 2). It is known that the interlayer distance of $Li_{1-y}NiO_2$ shrinks considerably at the end of charging [3]. This therefore suggests that the highly delithiated states of $Li_{1-y}NiO_2$ ($y > 0.8$) decomposed at 40°C and lead to a partial degradation of the material and thus the irreversible behavior. This unsatisfactory high-temperature performance of $Li_{1-y}NiO_2$ needs to be improved, in addition to the exothermal decomposition behavior at 200°C.

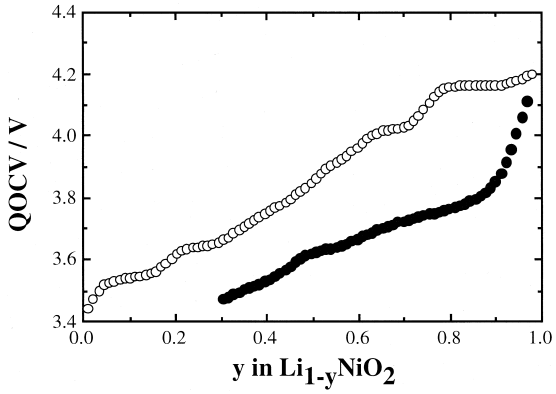

Fig. 2. QOCV profiles of $Li_{1-y}NiO_2$ during the first charge–discharge cycle at 40°C.

3.3. Characteristics of $LiNi_{0.9}M_{0.1}O_2$ (M = Co, Mn, Ti)

Partial substitution for nickel is the key to improving these undesirable properties. The amount of substitution must be kept to a minimum so as to maintain the large capacity of pristine $LiNiO_2$. We attempted a 10% substitution for nickel using cobalt, manganese and titanium as the substituents.

We evaluated the cycle performance of $LiNi_{0.9}M_{0.1}O_2$ (M = Co, Mn, Ti) at 20°C. The result is shown in Table 1. They all showed large cycle capacities, owing to the well-defined layered structures and the small amounts of substituent. The performance at 40°C was improved by introducing cobalt as the substituent. Although there was some irreversibility, the cobalt-substituted compound showed a large discharge capacity (corresponding to

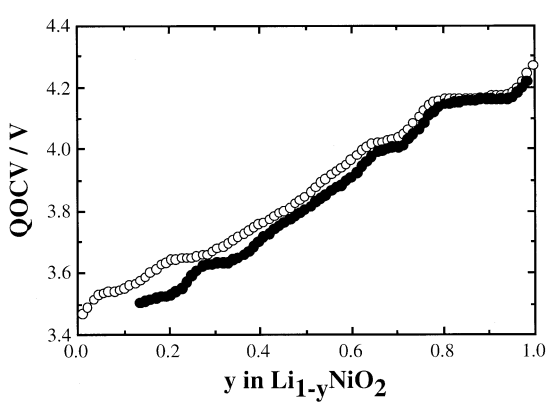

Fig. 1. QOCV profiles of $Li_{1-y}NiO_2$ during the first charge–discharge cycle at 20°C.

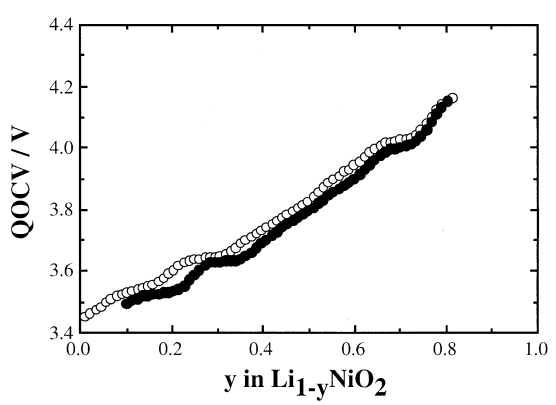

Fig. 3. QOCV profiles of $Li_{1-y}NiO_2$ at 40°C. The charging process was stopped at $Li_{0.2}NiO_2$ and was followed by the discharging process.

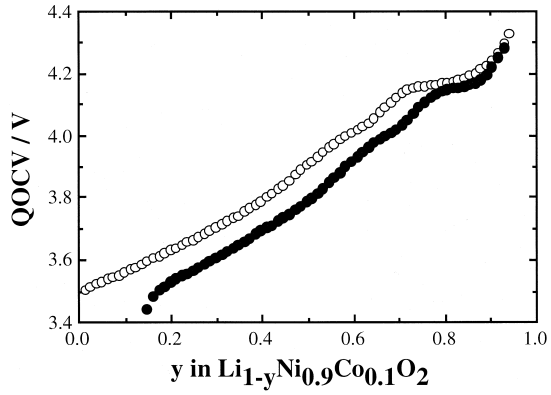

Fig. 4. QOCV profiles of $Li_{1-y}Ni_{0.9}Co_{0.1}O_2$ during the first charge–discharge cycle at 40°C.

220 mA h g^{-1}) at 40°C as shown in Fig. 4. As cobalt is oxidized later than nickel [27,28], the remaining Co^{3+} seems to contribute to the enhanced stability under our experimental conditions. The slanted voltage profile is useful for controlling the degree of delithiation using voltage detection. The manganese- and titanium-substituted compounds showed inadequate performance at 40°C. Fig. 5 shows the result for the manganese-substituted compound with about 60% of the material available during discharging. The titanium-substituted material behaved similarly.

Fig. 6 shows the thermal behavior of delithiated compounds measured by using DSC analysis. We fixed the degree of delithiation at $y = 0.8$ in $Li_{1-y}(TM)O_2$ for examining the thermal stability. It has been shown that $Li_{1-y}NiO_2$ generates the largest exothermal heat when y is around 0.8 [15]. While the cobalt-substituted compound behaved like $Li_{0.2}NiO_2$ with an exothermal peak at around 200°C, the manganese- and titanium-substituted compounds exhibited endothermal behavior, that is, they have better thermal stability. The thermal decomposition of $LiNiO_2$ results in a large amount of exothermal heat that

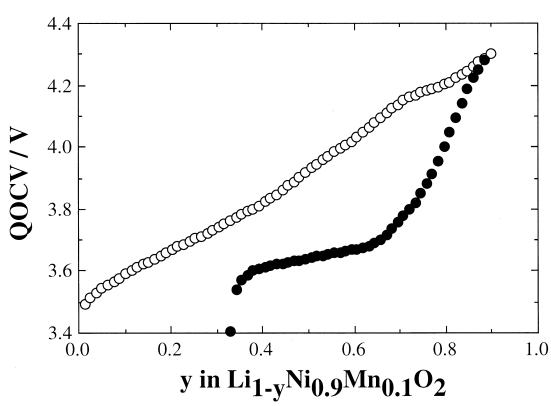

Fig. 5. QOCV profiles of $Li_{1-y}Ni_{0.9}Mn_{0.1}O_2$ during the first charge–discharge cycle at 40°C.

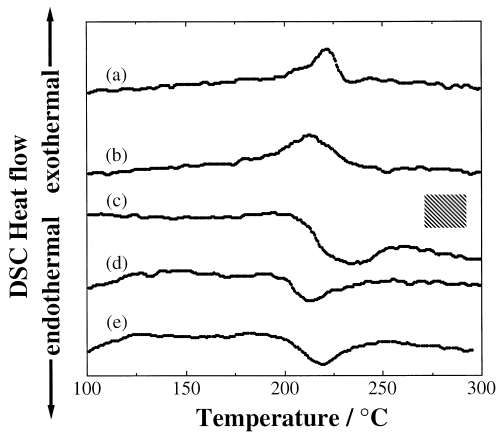

Fig. 6. DSC profiles of highly delithiated compounds at a heating rate of 10°C min^{-1}. (a) $Li_{0.2}NiO_2$, (b) $Li_{0.2}Ni_{0.9}Co_{0.1}O_2$, (c) $Li_{0.2}Ni_{0.9}Mn_{0.1}O_2$, (d) $Li_{0.2}Ni_{0.9}Ti_{0.1}O_2$, (e) $Li_{0.2}Ni_{0.8}Co_{0.1}Ti_{0.1}O_2$. The hatched area in the figure corresponds to heat of approximately 100 J g^{-1}.

originates in the disorderly mixing of the cations and a small amount of endothermal heat that originates in the oxygen evolution from the solid matrix [15]. Therefore, we believe that the exothermal heat was suppressed and only endothermal heat was observed with the manganese- and titanium-substituted materials. These two compounds differ structurally from $LiNiO_2$ (and the cobalt-substituted compound) in that their transition metal predominant layer contains lithium, and this structural characteristic seems to play a role in suppressing the exothermal heat. Further study is needed to clarify the details of the decomposition mechanism.

In conclusion, $LiNi_{0.9}M_{0.1}O_2$ (M = Co, Mn, Ti) performed better than the non-substitutive $LiNiO_2$, however, none of them succeeded in solving both problems, namely the irreversibility at 40°C and the exothermal behavior at around 200°C.

3.4. Characteristics of $LiNi_{0.8}Co_{0.1}M_{0.1}O_2$ (M = Mn, Ti)

The results in the preceding section urged us to study the characteristics of the doubly substituted system $LiNi_{0.8}Co_{0.1}M_{0.1}O_2$ (M = Mn, Ti). We again kept the amount of substitution at 10% for each substituent.

Table 1 shows that $LiNi_{0.8}Co_{0.1}Ti_{0.1}O_2$ showed a larger cycle capacity at 20°C than $LiNi_{0.8}Co_{0.1}Mn_{0.1}O_2$. This is probably because our $LiNi_{0.8}Co_{0.1}Mn_{0.1}O_2$ powder was quite coarse, compared with the fine $LiNi_{0.8}Co_{0.1}Ti_{0.1}O_2$ powder. Another reason could be the structural characteristics of the sample. Although the *x* and *w* values are similar in both samples, the lattice parameters are quite different as shown in Table 1. More detailed analysis, for example that using neutron diffraction analysis, is needed to clarify structural factors which determine the electrochemical performance. Here we focused on the more attractive compound, $LiNi_{0.8}Co_{0.1}Ti_{0.1}O_2$.

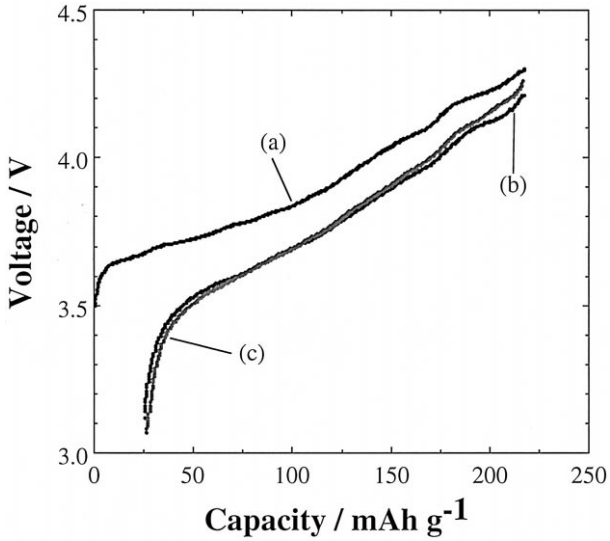

Fig. 7. Cycle profile of $LiNi_{0.8}Co_{0.1}Ti_{0.1}O_2$ at 20°C and at 0.5 mA cm^{-2}. (a) First charging, (b) first discharging, (c) 10th discharging profiles.

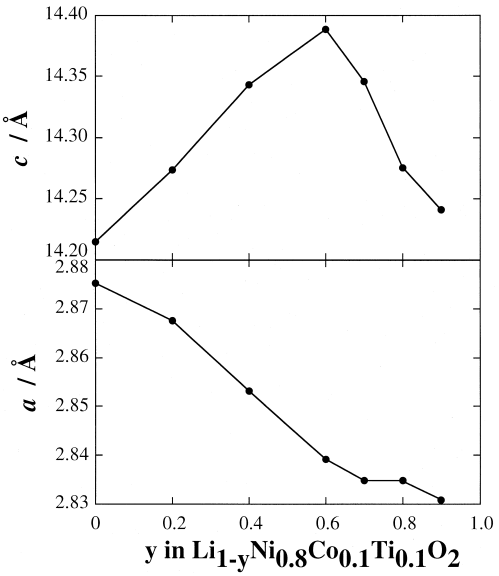

Fig. 9. Hexagonal unit cell parameters of $Li_{1-y}Ni_{0.8}Co_{0.1}Ti_{0.1}O_2$ during charging. Data points are interpolated for clarity.

The cycle profiles at 20°C are shown in Fig. 7, indicating its good cyclablity. Fig. 8 shows the good reversibility of $LiNi_{0.8}Co_{0.1}Ti_{0.1}O_2$ at 40°C which is close to that of $LiNi_{0.9}Co_{0.1}O_2$ shown in Fig. 4. We observed the endothermal decomposition of $Li_{0.2}Ni_{0.8}Co_{0.1}Ti_{0.1}O_2$ which is similar to that of $Li_{0.2}Ni_{0.9}Ti_{0.1}O_2$, as shown in Fig. 6.

We examined the structural changes of $Li_{1-y}Ni_{0.8}Co_{0.1}Ti_{0.1}O_2$ during charging. Fig. 9 shows the structural parameters of several charged (delithiated) samples. The hexagonal unit cell parameter *a* monotonously decreased while *c* was maximum at $Li_{0.4}Ni_{0.8}Co_{0.1}Ti_{0.1}O_2$. This behavior is similar to that of $Li_{1-y}Ni_{0.9}Co_{0.1}O_2$ [18]. Unlike $Li_{1-y}NiO_2$, $Li_{1-y}Ni_{0.8}Co_{0.1}Ti_{0.1}O_2$ showed no considerable interlayer shrinkage (one-third of the *c*-axis length) which would deteriorate the material. Accordingly, this doubly substituted nickelate $LiNi_{0.8}Co_{0.1}Ti_{0.1}O_2$ is promising as an electrode material with a large capacity, enhanced high-temperature performance, and good thermal stability.

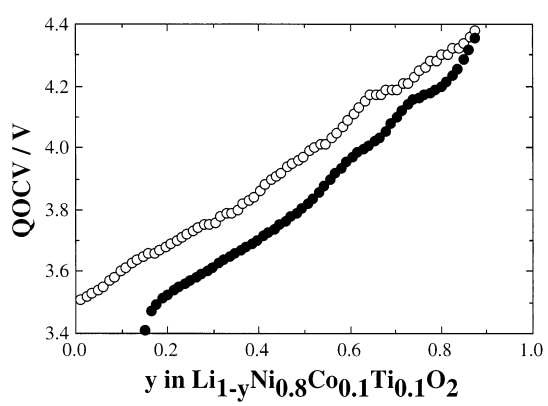

Fig. 8. QOCV profiles of $LiNi_{0.8}Co_{0.1}Ti_{0.1}O_2$ during the first charge–discharge cycle at 40°C.

4. Conclusions

$LiNiO_2$ and its partially substituted compounds show large capacities of about 200 mA h^{-1} at 20°C when the transition metal content is low in the lithium predominant layer. When fully delithiated, $LiNiO_2$ shows irreversible behavior at 40°C. Highly delithiated compounds (e.g. $Li_{0.2}NiO_2$) decompose exothermally at around 200°C. The reversibility at 40°C is improved by introducing cobalt as a partial substituent for nickel. Manganese and titanium substitution is effective in improving the thermal stability at 200°C. The doubly substituted nickelate $LiNi_{0.8}Co_{0.1}Ti_{0.1}O_2$ exhibited a large capacity, enhanced high-temperature performance, and good thermal stability in the delithiated state.

Acknowledgements

The authors express their gratitude to Dr. Ichiro Yamada for his encouragement during the course of this research. The authors are also grateful to Ms. Noriko Kurusu and Mr. Ryuichi Nishio (both of NTT Advanced Technology) for their excellent technical support.

References

[1] M.G.S.R Thomas, W.I.F. David, J.B. Goodenough, Mater. Res. Bull. 20 (1985) 1137–1146.

[2] J.R. Dahn, U. von Sacken, C. A. Michal, Solid State Ionics 44 (1990) 87–97.
[3] T. Ohzuku, A. Ueda, M. Nagayama, J. Electrochem. Soc. 140 (1993) 1862–1870.
[4] W. Li, J.N. Reimers, J.R. Dahn, Solid State Ionics 67 (1993) 123–130.
[5] M. Broussely, F. Perton, J. Labat, R.J. Staniewicz, A. Romero, J. Power Sources 43–44 (1993) 209–216.
[6] W. Ebner, D. Fouchard, L. Xie, Solid State Ionics 69 (1994) 238–256.
[7] A. Hirano, R. Kanno, Y. Kawamoto, Y. Takeda, K. Yamaura, M. Takano, K. Ohyama, M. Ohashi, Y. Yamaguchi, Solid State Ionics 78 (1995) 123–131.
[8] H. Arai, S. Okada, H. Ohtsuka, M. Ichimura, J. Yamaki, Solid State Ionics 80 (1995) 261–269.
[9] R.V. Moshtev, P. Zlatilova, V. Manev, A. Sato, J. Power Sources 54 (1995) 329–333.
[10] A. Rougier, P. Gravereau, C. Delmas, J. Electrochem. Soc. 143 (1996) 1168–1175.
[11] H. Arai, S. Okada, Y. Sakurai, J. Yamaki, Solid State Ionics 95 (1997) 275–282.
[12] J.R. Dahn, E.W. Fuller, M. Obrovac, U. von Sacken, Solid State Ionics 69 (1994) 265–270.
[13] T. Ohzuku, A. Ueda, M. Kouguchi, J. Electrochem. Soc. 142 (1995) 4033–4039.
[14] D. Wainwright, J. Power Sources 54 (1995) 192–197.
[15] H. Arai, S. Okada, Y. Sakurai, J. Yamaki, Solid State Ionics 109 (1998) 295–302.
[16] Z. Zhang, D. Fouchard, J.R Rea, J. Power Sources 70 (1998) 16–20.
[17] H. Arai, Y. Sakurai, J. Power Sources 81–82 (1999) 401–405.
[18] H. Arai, S. Okada, Y. Sakurai, J. Yamaki, J. Electrochem. Soc. 142 (1997) 3117–3125.
[19] Y. Gao, M.V. Yakovieva, W.B. Ebner, Electrochem. Solid State Lett. 1 (1998) 117–119.
[20] F. Izumi, R.A. Young (Eds.), The Rietveld Method, Oxford Univ. Press, Oxford, 1993, p. 236.
[21] C. Delmas, I. Saadoune, Solid State Ionics 53–56 (1992) 370–375.
[22] T. Ohzuku, A. Ueda, M. Nagayama, Y. Iwakoshi, H. Komori, Electrochim. Acta 38 (1993) 1159–1167.
[23] A. Rougier, I. Saadoune, P. Gravereau, P. Willmann, C. Delmas, Solid State Ionics 90 (1996) 83–90.
[24] E. Rossen, C.D.W. Jones, J.R. Dahn, Solid State Ionics 57 (1992) 311–318.
[25] M. Yoshio, Y. Todorov, K. Yamato, H. Noguchi, J. Itoh, M. Okada, T. Mouri, J. Power Sources 74 (1998) 46–53.
[26] D. Caurant, N. Baffier, V. Bianchi, G. Gregoire, S. Bach, J. Mater. Chem. 6 (1996) 1149–1155.
[27] I. Saadoune, C. Delmas, Solid State Ionics 136 (1998) 8–15.
[28] T. Nakagome, I. Nakai, Denki Kagaku 66 (1998) 727–733.